

The angular momentum of $1.2M_{\odot}$ to $2.0M_{\odot}$
main-sequence and turn-off stars constrain the
relationship between star-forming environment
and galactic evolution history

Yu-Fu Shen¹, Yan Xu^{1,2}, Yi-Bo Wang¹, Xiu-Lin Huang¹,
Xing-Xing Hu¹, Qi Yuan¹

¹Changchun Observatory, National Astronomical Observatories, Chinese
Academy of Sciences, Jilin, China.

²School of Astronomy and Space Science, University of Chinese
Academy of Sciences, Beijing, China.

Contributing authors: shenyf@cho.ac.cn;

Abstract

Kepler and *Gaia* data shows an anomaly in the angular momentum-age relationship for 1.2-2 main-sequence stars. After considering model-induced correlation of parameters, the moment of inertia, stellar velocity distribution, sample selection effects, interactions between the Milky Way and dwarf galaxies, the star-disk interaction during the early pre-main sequence, and the angular momentum change on the main sequence, this work suggests that the earlier the star within this mass range born, the smaller the angular momentum at the time of born, following an exponential decay relationship. This relationship should be attributed to the variation in molecular cloud parameters throughout the history of the Milky Way.

Keywords: moment of inertia, stellar evolutionary models, initial mass function, substructure: galaxy

1 Main

The angular momentum of molecular clouds is much larger than that of stars. However, the rotation speed of stars typically remains below the breakup speed, with one of the main breaking mechanisms being the star-disk interaction during the early pre-main sequence (PMS[1–6]). In addition, gravitational torques also prevent a star from spinning faster than approximately 50% of its breakup speed during formation [7]. Lower-mass stars are more strongly affected by the breaking mechanism, with speeds roughly at 10% of the breakup speed[8, 9], while higher-mass stars have speeds above 20% to 40% [10, 11], partly due to the disk-clearing accretion phase significantly reducing the stellar angular momentum, and massive stars are more difficult to spin down in the disk-clearing phase due to their larger inertia and weaker magnetic fields[12].

This work mainly analyzes samples with masses between $1.2M_{\odot}$ and $2M_{\odot}$, which is called the target sample. The distribution of RR/P , radius times radius (R_{\odot}) divided by rotation period (day), versus age for 33,601 stars, obtained by cross-referencing the rotation period from *Kepler*[13, 14] with *Gaia* DR3[15–17], shows that RR/P for stars with masses below about $1.2M_{\odot}$ remain within the range of 0.1-0.01 from zero age to approximately 12 Gyr (Fig. 1). This aligns with current observations: on the one hand, there is a roughly 30-fold difference in rotation speeds among low-mass stars at birth[18–32], and it can be assumed that the angular momentum distribution is similar; on the other hand, the rate of angular momentum loss due to stellar winds is negligible compared to the total angular momentum of a star[33], so the RR/P distribution of low-mass stars in Fig. 1 changes little over time. However, the RR/P of the target sample in Fig. 1, which is divided into two categories (turn-off and main sequence, the basis for classification is explained in detail later), is larger than that of less massive stars, which is normal, but it also has a nearly two-order-of-magnitude decay with age, which is abnormal. However, the RR/P -age relationship is likely not a reflection of the evolution of angular momentum with age, but rather a manifestation of the stellar mass-age relationship, as the age span of the target sample exceeds the main-sequence lifetime of stars with $2M_{\odot}$ (approximately 1 Gyr). Fortunately, stars of a small mass range within the sample also exhibit a wide range of age distributions, besides there is a significant difference in main-sequence and turn-off masses for stars of the same age, yet they share a similar RR/P -age relationship, and Fig. 2 is an example. After the main-sequence phase of a star ends, it enters the turn-off phase, during which both its radius and rotational speed undergo abrupt changes, while angular momentum remains conserved, allowing it to maintain a consistent angular momentum-age distribution with that of the main-sequence phase. Incidentally, abrupt changes in the moment of inertia will increase the difference between RR/P and the angular momentum, which will be discussed in detail later. We believe that the RR/P -age relationship is not solely a representation of the stellar mass-age relation but rather hints at deeper underlying physics. This work aims to understand the RR/P -age relationship.

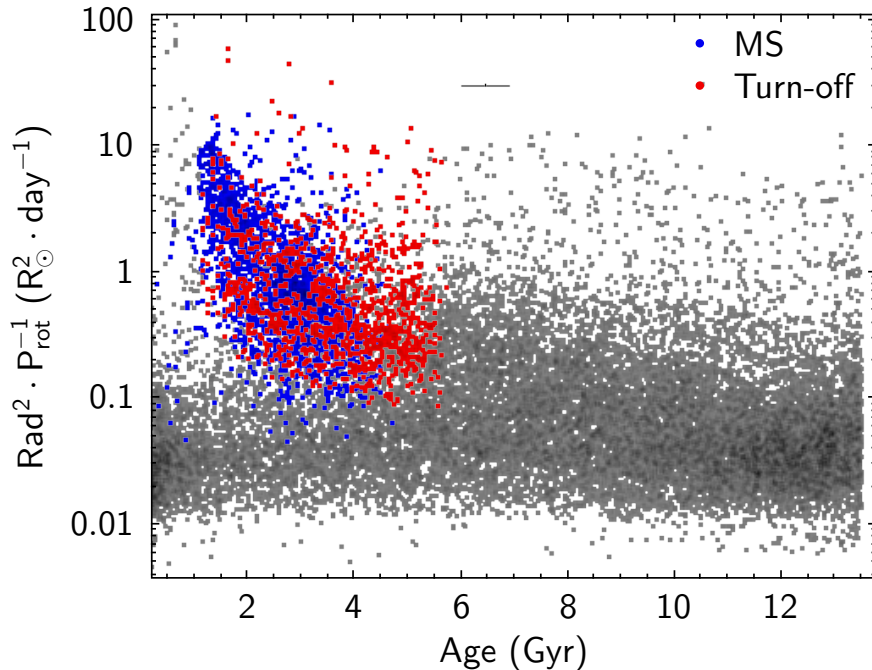


Fig. 1 The figure shows the RR/P -age distribution for Kepler targets with rotation period. The non-target samples are colored gray, while the target samples ($1-1.2M_{\odot}$) are divided into main-sequence (blue) and turn-off (red). The cross at the top center of the figure indicates the average error range for the target samples, where the average error for RR/P is $0.35 (M_{\odot}^2 \cdot \text{day}^{-1})$.

1.1 Rule out systematic errors in parameters and model-induced correlation

In Fig. 3, both the age and stellar radius are derived from *Gaia*'s Final Luminosity Age Mass Estimator (FLAME¹) program, which uses the GSP-Phot parameters² as input. GSP-Phot parameters are determined based on BP/RP spectra, G magnitude, and parallax. BP/RP spectra that can lead to errors in the $\log g$ estimations, where $\log g$ has a significant impact on stellar radius. However, GSP-Phot parameters also take into account parallax and apparent magnitude, allowing the calculation of absolute magnitude, which significantly reduces the error in $\log g$ and facilitates the identification of binaries. At this point, if there are errors in the parameters, they may be due to the accuracy of the G magnitude and parallax. Fig. 4 shows that the distribution of errors in G magnitude and parallax for the target is smaller than that of the overall sample because of the brighter nature of the target stars. Therefore, the GSP-Phot parameters in this sample are reliable.

¹https://gea.esac.esa.int/archive/documentation/GDR3/Data_analysis/chap_cu8par/sec_cu8par_apsis/ssec_cu8par_apsis_flame.html

²https://gea.esac.esa.int/archive/documentation/GDR3/Gaia_archive/chap_datamodel/sec_dm_astrophysical_parameter_tables/ssec_dm_astrophysical_parameters.html

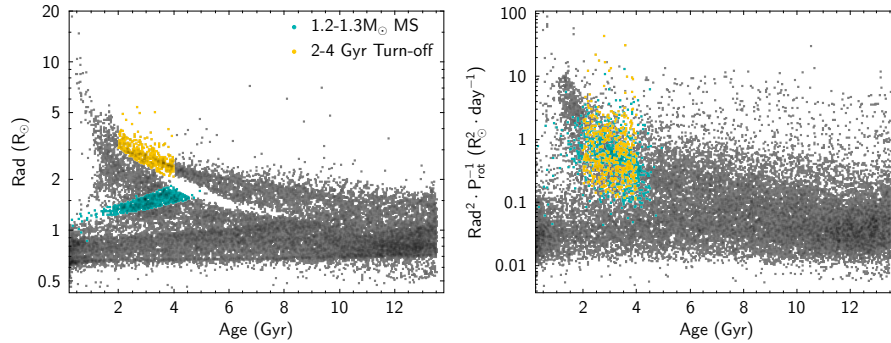


Fig. 2 The left panel is a radius-age diagram, while the data in the right panel are consistent with Fig. 1, and the highlighted samples are the same as those in the left panel. The mean error of the radii for main-sequence samples is 0.08, and the mean error of the radii near the turn-off region of the age range is 0.25 Gyr.

Taking into account the overly apparent correlation between `Age_Flame` and `Rad_Flame` in Fig. 3, it is likely a case of model-induced correlation. `Rad_Flame` is directly derived from the GSP-Phot parameters and absolute magnitude based on the Stefan-Boltzmann equation. The reliability of the GSP-Phot parameters was discussed in the previous paragraph, and thus `Rad_Flame` can be deemed reliable. However, `Age_Flame` is determined by FLAME through Monte Carlo simulations based on stellar parameters. Given that stellar age may exhibit degeneracy in the stellar parameter space, there is a possibility of model-induced correlation leading to complete distortion of age. Fortunately, Fig. 5 shows that for the target samples, there is a positive correlation between age and rotation period. There cannot be a model-induced correlation between rotation period and age, as will be discussed in the last paragraph of this subsection. Therefore, age is at least statistically reliable, which means that the distribution of RR/P -age cannot be solely attributed to model-induced correlation.

It must be said that the FLAME parameters are imperfect. As shown in Fig. 6, there exists a gap between the red and blue samples; at the same mass, the red samples are older, but FLAME seems to set an upper limit of $10 \cdot M^{-2.9}$ for age, which roughly corresponds to the theoretical upper limit for the age of stars in the main-sequence phase, so it is a model-induced correlation. This might be due to the difficulty in estimating the ages of stars in the turn-off phase. This also implies that the ages of the red target samples may be underestimated. However, the turn-off phase for stars in this mass range is currently believed to typically last much less than 1Gyr [34], which should not introduce significant errors in age estimation. Therefore, in this work, the targets are classified into two categories: the turn-off phase (red) and the main-sequence phase (blue). This work segments the samples on the basis of the mass-radius diagram, and the specific segmentation is provided in the Appendix.

In addition, binaries could affect the result. *Gaia* also provides the probability from DSC-Combmod of being binary star³. As seen in Fig. 7, the proportion of suspected binaries in the sample is extremely low. As previously mentioned, the parallax errors

³https://gea.esac.esa.int/archive/documentation/GDR3/Gaia_archive/chap_datamodel/sec_dm_astrophysical_parameter_tables/ssc_dm_astrophysical_parameters.html

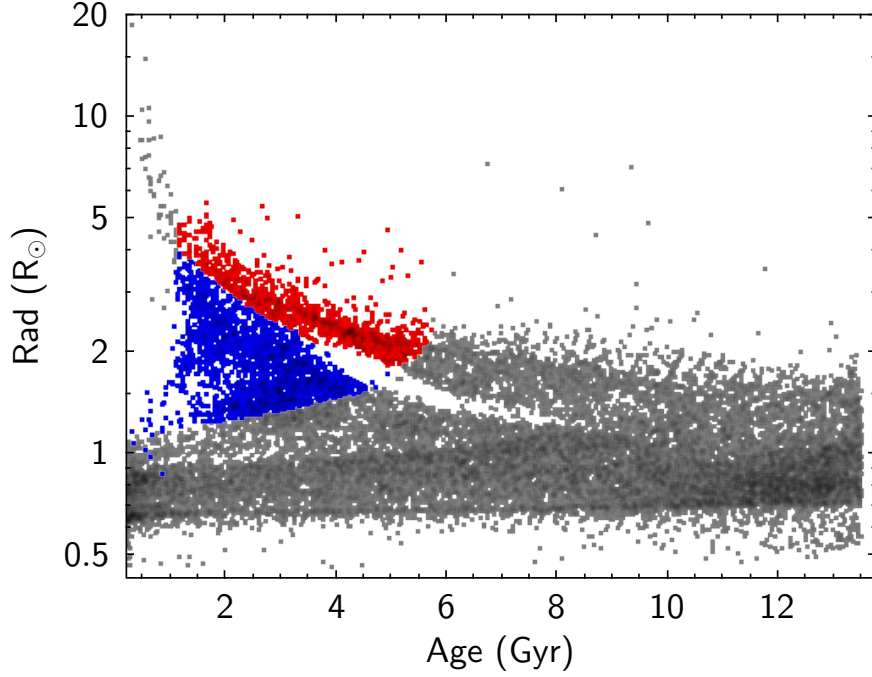


Fig. 3 Age-radius diagram of the sample. Unless otherwise specified, the meaning of colors in all figures in this paper is consistent with Fig. 1. The mean error of the radii for turn-off stars is $0.22R_{\odot}$, and the mean error of the radii for main-sequence stars is $0.122R_{\odot}$.

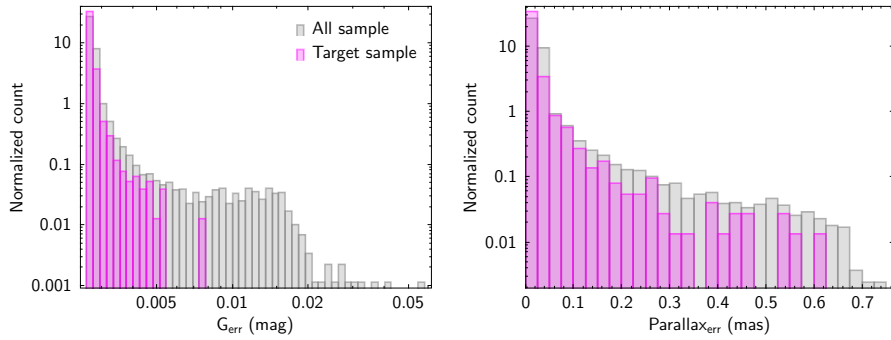


Fig. 4 The distribution of G magnitude errors and parallax errors for both the total sample and the target sample.

and G-magnitude errors in the sample are both relatively small, so unless the companion star is faint and lacks interaction between the host star, the binaries can be identified through its absolute magnitude. The probability of being binary provided by *Gaia* should be reliable in this case. Therefore, the impact of binaries is not discussed further in this work.

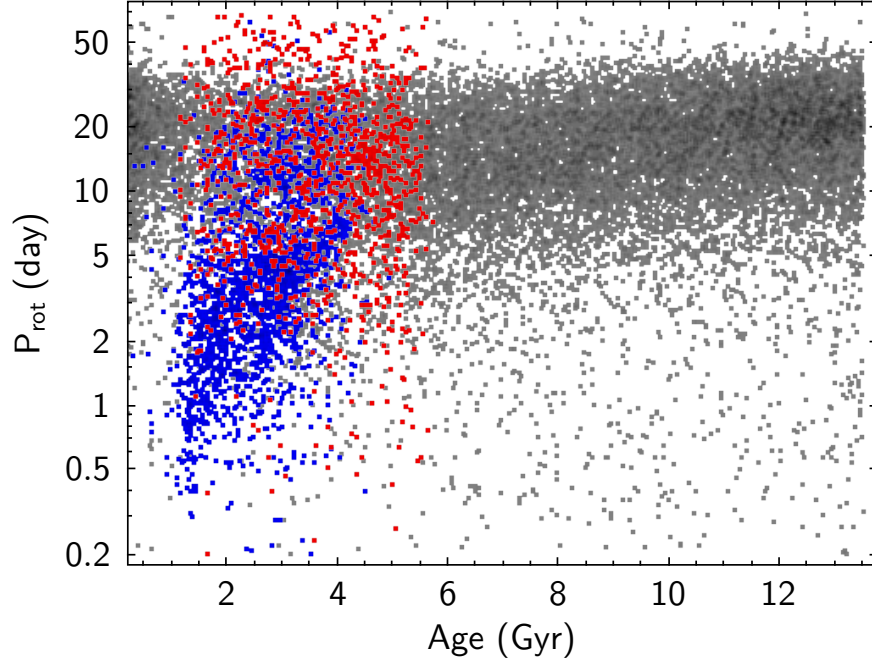


Fig. 5 The rotation period-age distribution of the samples. The average error in the rotation period of the target samples is 0.36 days.

Based on the above discussion, when we revisit Fig. 1, it can be observed that the gap between the turn-off and the main sequence completely disappears when the y axis is changed to RR/P from R . Firstly, this cannot be the result of the model-induced correlation canceling each other out, because P_{rot} is derived from *Kepler* light curve, has a four-year duration and obtained by McQuillan et al. 2014[35] using the autocorrelation method. P_{rot} can be considered highly accurate, and there cannot be a model-induced correlation between it and `Age_Flame` or `Rad_Flame`. The gap between the turn-off and the main sequence is caused by abrupt changes in stellar structure at the end of the main sequence phase, this implies an abrupt change in moment of inertia. The observed rotational periods of turn-off stars are generally low, which happens to maintain the conservation of angular momentum, thereby causing the gap between the turn-off and the main sequence to disappear. This suggests that turn-off and main-sequence stars of the same age in the target sample not only have similar angular momentum but also follow similar angular momentum-age relationships. This subset of samples is very useful for studying structural changes in stars entering the turn-off stage, although the focus of this work is not on studying stellar structure. The focus of this work lies in understanding why turn-off and main-sequence stars in the target sample possess the same angular momentum-age relationship.

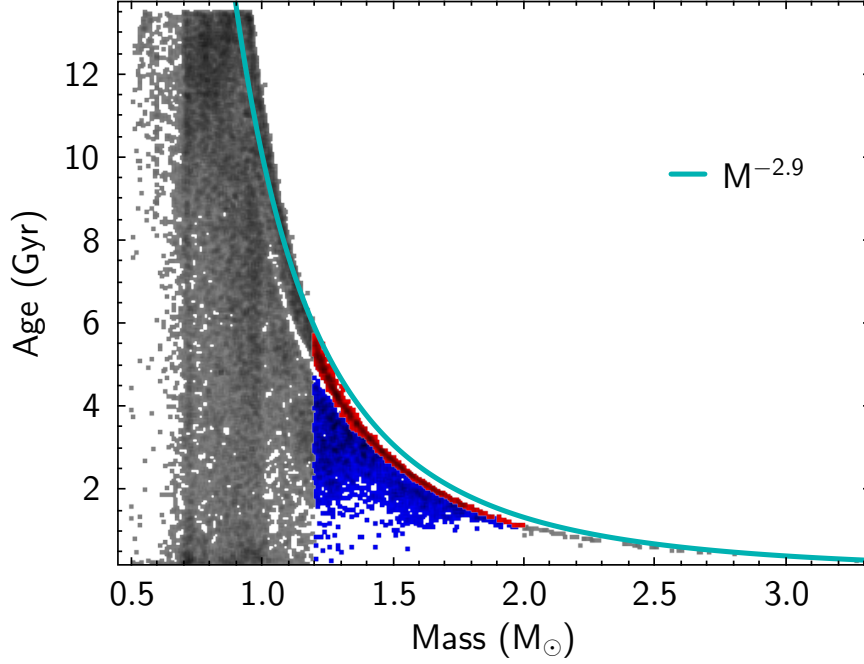


Fig. 6 Age-mass diagram of the sample. This diagram aims to show that the FLAME program seems to set an upper limit according to the theoretical main-sequence age.

1.2 Assess the influence of the moment of inertia and stellar velocity distribution

In reality, RR/P is not an angular momentum L . $L \propto I/MR^2 \cdot M \cdot RR/P$, where I is the moment of inertia. The masses of the target sample are all within 1 to 2 M_{\odot} , with an impact far less than an order of magnitude. I/MR^2 for a uniform sphere is 0.4, while for the Sun it is 0.07⁴. Calculations in Claret & Gimenez 1989[36] show that for masses ranging from 1 to 2.5 M_{\odot} and ages up to 10 Gyr, I/MR^2 falls between 0.026 and 0.147, with the maximum impact also less than an order of magnitude. However, after entering the turn-off phase, there is not yet a well-established theoretical model to describe the changes in I/MR^2 , but it is expected that I/MR^2 will be smaller because more masses concentrate to the core. In this case, the angular momentum-age distribution of the red target sample should be lower than the RR/P -age distribution, which makes the distributions of the red and blue target sample closer to each other.

In addition, stars also exhibit differential rotation. The rotation rates provided by *Kepler* data are obtained by detecting quasi-periodic brightness variations, which arise as magnetically active regions on the star's surface rotate in and out of view. The resulting rotation period should be close to the period at the latitude where sunspots most frequently appear, which is around 16 degrees for the Sun. This is not the typical rotation rate on the Sun's surface, but the impact is minor because the maximum

⁴<https://nssdc.gsfc.nasa.gov/planetary/factsheet/sunfact.html>

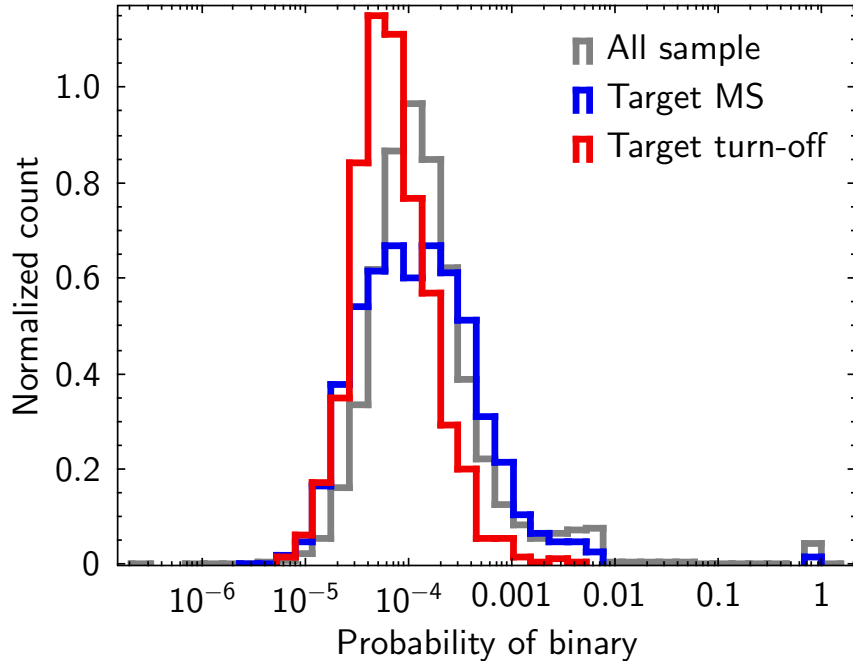


Fig. 7 The distribution of the probability that an object in the sample is a binary.

difference in the surface rotation period of the Sun is only approximately a factor of 1.4[37]. In addition, the velocity distribution within the star also differs. When deeper than the tachocline, at the base of the convection zone, the rotation period at various latitudes of the star tends to converge approaching the rotation rate at about 30 degrees latitude at the surface, as in the case of the Sun[37]. The masses of target sample in this work do not exceed the Sun by much, so it should be appropriate to use solar parameters for estimation.

In summary, within the framework of existing theories and observational data, the observed phenomena in this work are unlikely to be strongly biased by uncertainties arising from the velocity distribution. The moment of inertia may have a stronger impact than the velocity distribution, but it will not be larger than one magnitude.

1.3 Rule out the selection effect

It is necessary to determine whether the samples in this work are representative. Longer-period rotation is generally more difficult to detect for two reasons. Firstly, longer-period rotation requires observational data that span a longer period of time, but the *Kepler* data span up to four years, so the impact of this aspect can be ignored. Secondly, the magnetic activity of slower rotating stars is weaker, making the variations in their light curves less pronounced. In addition, massive stars exhibit a more severe selection bias compared to solar-like stars because their magnetic activity is weaker. So, selection bias resulting in the omission of slowly rotating target sample stars. Fig. 8

shows the mass distribution of the sample and that of all *Kepler* samples, indicating that a selection effect does indeed exist, but the target sample can still represent at least half of the stars within the same mass range in the overall sample. Moreover, even if a large number of slowly rotating massive stars were omitted, they would only be added below the target sample in Fig. 1, and the clear trend of RR/P -age at the upper side of the distribution would remain unchanged.

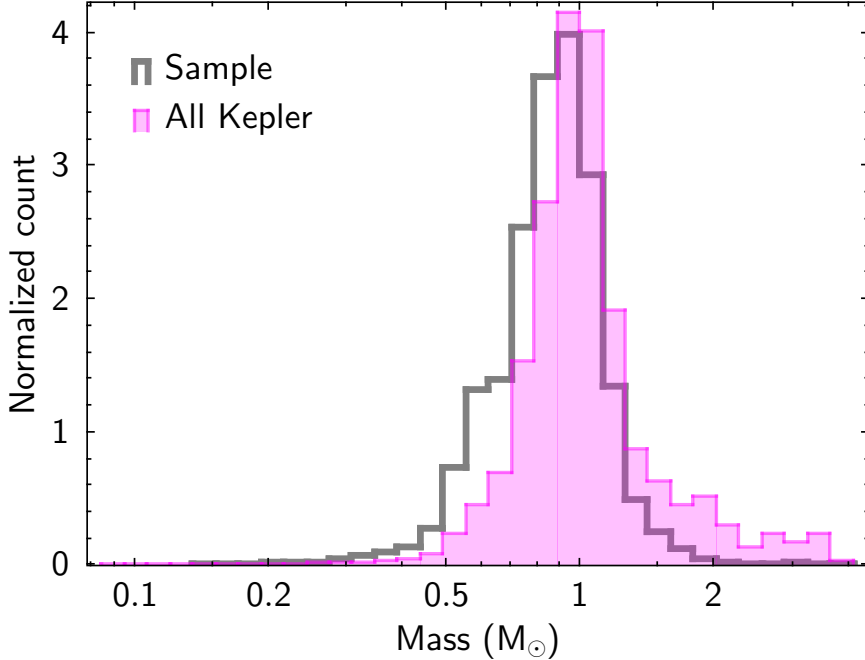


Fig. 8 The mass distribution of all *Kepler* targets and *Kepler* targets with rotation periods. For consistency, the masses in this plot are provided by *Kepler* catalog. This figure is intended to qualitatively demonstrate the selection effects of rotation period measurements.

1.4 Rule out the interactions between the Milky Way and dwarf galaxies

For stars accreted by the Milky Way, their formation environments differ significantly from those of field stars in the Milky Way. If the samples originate from outside the Milky Way, more explanations can be considered. A star cluster in or near the Galaxy initially exhibited clustering properties; through interaction with the Galaxy, it gradually disintegrates and forms a stellar stream [38–41]; subsequently, it loses spatial distribution characteristics and retains only kinematic features, such as the Gaia sausage [42]. Based on the proper motion, parallax and radial velocity provided by *Gaia* DR3 [15, 17], Galactic space-velocity components [43] and orbital elements under the McMillan17 gravitational potential [44] are calculated. The results in Fig. 9

indicate that the samples lack distinct kinematic characteristics; Fig. 10 indicate that the samples appear to not have clusters. The sample can be considered to be field stars within the Galactic disk.

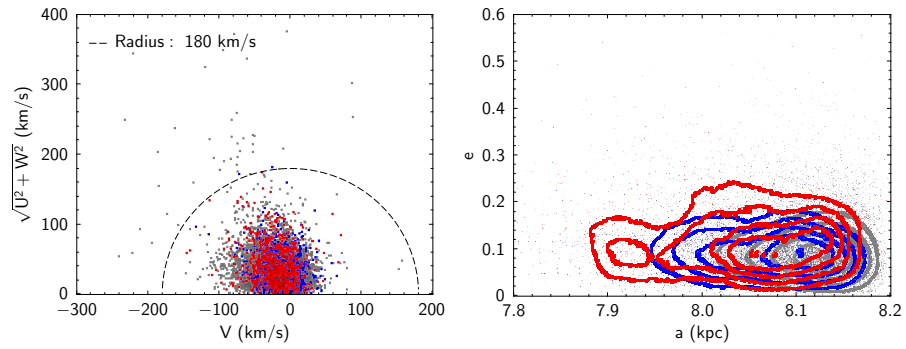


Fig. 9 The distribution of samples in the kinematic parameter space. The dashed line in the left figure outlines the approximate range of the Galactic disk.

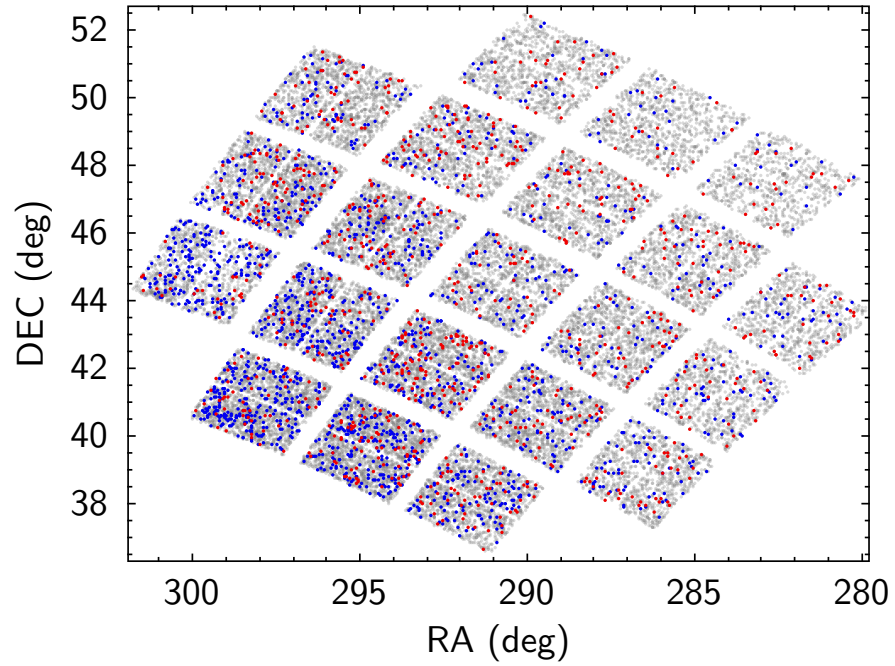


Fig. 10 The sky location of the sample.

1.5 Star-disk interaction during the pre-main sequence

The angular momentum of the target samples is 2 to 3 orders of magnitude higher than that of low-mass stars, prompting us to first consider the source of their initial angular momentum. The initial angular momentum of stars is inherited from molecular clouds but undergoes significant removal during star-disk interaction in the PMS. According to Rosen et al. 2012[12], for stars of the same mass, the varying parameters (Section 4.2 in Rosen et al. 2012) have a minor impact on their radii, but the varying parameters significantly influence the stellar rotation period, which could reach 2 to 3 orders of magnitude. This indicates that by adjusting parameters during the PMS phase, such as the properties of molecular clouds, the observed angular momentum distribution, only in terms of numerical values, can be explained. However, the angular momentum of the target samples decreases with age, dropping by nearly two orders of magnitude within 3-4 Gyr, which needs further explanation.

1.6 Angular momentum change during the main sequence

The change in angular momentum during the main-sequence phase of stars is primarily due to stellar wind losses and redistribution of angular momentum. The latter essentially involves changes in the distribution of rotational velocity and moment of inertia, which have been discussed in Sec. 1.2. The influence of moment of inertia does not reach an order of magnitude, and the impact of the distribution of rotational velocity is even smaller, making it impossible to explain the angular momentum loss of nearly two orders of magnitude. Taking into account the effect of mass and age, further filtering can be performed on target samples by restricting the mass to a narrower range, as shown in Fig. 2. It can be observed that there is still a one-order-of-magnitude decrease within a few Gyr. If this is caused by stellar wind losses, J_*/\dot{J}_* should be within a few Gyr. For the sun, $J_\odot = 2 \cdot 10^{48}$ c.g.s. and $\dot{J}_\odot = 2 \cdot 10^{29}$ c.g.s., and $\dot{J}_\odot \cdot 1\text{Gyr} = 6 \cdot 10^{45}$ c.g.s. So,

$$\frac{J_\odot}{\dot{J}_\odot} = 300\text{Gyr} \quad (1)$$

According to the scaling law in Cohen & Drake 2014[], $\dot{J}_* \propto B_*/P_*$ where B is the stellar magnetic field strength. $J_* \propto (I/MR^2)_* \cdot M_* \cdot R_* R_*/P_*$, so

$$\frac{J_*}{\dot{J}_*} = \frac{J_\odot}{\dot{J}_\odot} \cdot \frac{(I/MR^2)_* \cdot M_* \cdot R_*^2 \cdot B_*^{-1}}{(I/MR^2)_\odot \cdot M_\odot \cdot R_\odot^2 \cdot B_\odot^{-1}} \quad (2)$$

$M_* > 1.2M_\odot$ so $R_* > R_\odot$, $B_* < B_\odot$. To minimize J_*/\dot{J}_* , let $(I/MR^2)_*/(I/MR^2)_\odot = 0.026/0.07 = 0.37$, $M_*/M_\odot = 1.2$, $R_*^2/R_\odot^2 = 1$ and $B_*^{-1}/B_\odot^{-1}=1$, so

$$\min\left(\frac{J_*}{\dot{J}_*}\right) = 133\text{Gyr} \quad (3)$$

Therefore, stellar wind losses cannot explain the temporal variation of angular momentum in the target sample.

2 Discussion and conclusion

After considering systematic errors in parameters and model-induced correlation, the influence of the moment of inertia and stellar velocity distribution, selection effect, interactions between the Milky Way and dwarf galaxies, star-disk interaction during the pre-main sequence (PMS), and angular momentum change during the main sequence, this work concludes that the observed temporal variation in angular momentum for the $1.2\text{-}2M_{\odot}$ sample is due to their angular momentum at formation following this trend. An important piece of evidence is that turn-off stars and main-sequence stars of the same age but with significantly different radii within the $1.2\text{-}2$ mass range have similar angular momenta. This serves as an important reference for the evolutionary history of the Milky Way over the past approximately 5 Gyr. The theory framework allows us to explain angular momentum variations of 2-3 orders of magnitude by adjusting parameters during the PMS phase, such as adjusting the properties of molecular clouds. Therefore, this suggests that there is a certain regularity in star-forming regions within the Milky Way over the past approximately 5 Gyr, where older gas clouds form stars with smaller angular momentum, possibly following an exponential pattern. This pattern includes the following parameters: the average RR/P ($M_{\odot}^2 \cdot \text{day}^{-1}$), $RR_P(t_0)$ for newly formed $1.2\text{-}2$ solar mass stars in the Milky Way at a certain time t_0 (Gyr). Temporarily, it is recommended to use $t_0 = 1.2$, $\log RR_P(1.2) = 1$; the average RR/P , for $1.2\text{-}2M_{\odot}$ stars formed more than about 5 Gyr ago (RR_p^{∞}). The recommended value is $\log RR_p^{\infty} = -1.5$. Finally, there is a constant $c > 0$, which is related to the evolutionary pattern of the properties of molecular clouds in the history of the Milky Way. Based on the above parameters, the following empirical formula is given and the fit is shown in Fig. 11.

$$\log RR_P(\text{age}) = (\log RR_P^0 - \log RR_p^{\infty}) \cdot e^{-c(\text{age} - t_0)} + \log RR_p^{\infty} \quad (4)$$

The idea that $1.2\text{-}2M_{\odot}$ stars formed by older molecular clouds have a smaller angular momentum reminds us of the initial mass function (IMF) problem. Several observations and theories suggest that the IMF slope for massive stars in globular clusters (GCs) depends on the initial cloud density and metallicity (Z). The IMF becomes increasingly top-heavy with decreasing Z and increasing gas density[45]. If field stars also follow this pattern, considering that clouds in younger galaxy typically have lower Z and higher gas density, such clouds are likely to result in lower angular momentum of stars as well. If the properties of clouds with higher Z and lower density could lead to excessively higher angular momentum during the PMS stage, it would promote fragmentation and hinder the formation of more massive stars, strengthening the top-heavy phenomenon.

Acknowledgements. This work has made use of data from the European Space Agency (ESA) mission *Gaia* (<https://www.cosmos.esa.int/gaia>), processed by the *Gaia* Data Processing and Analysis Consortium (DPAC, <https://www.cosmos.esa.int/web/gaia/dpac/consortium>). Funding for the DPAC has been provided by national institutions, in particular the institutions participating in the *Gaia* Multilateral Agreement.

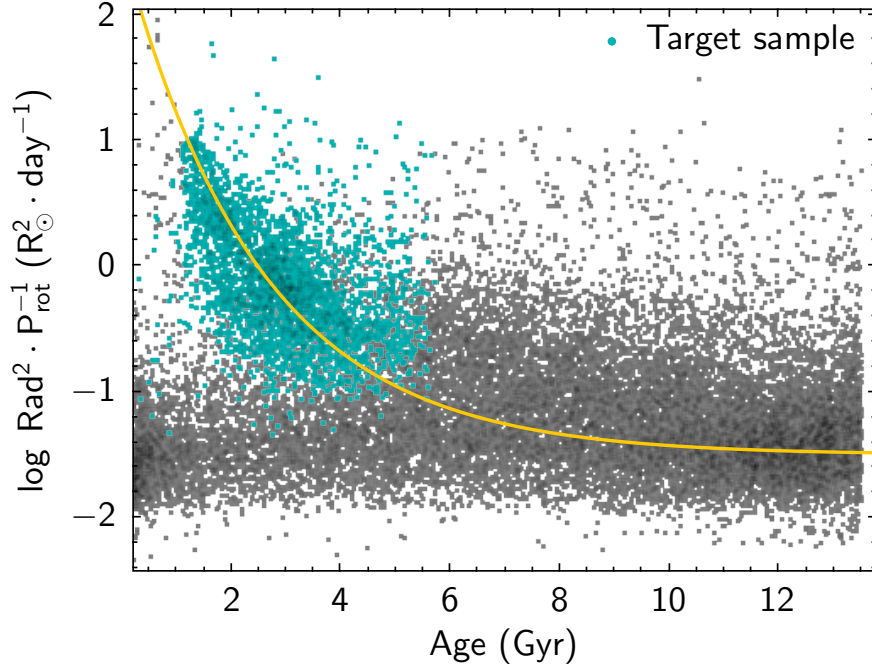


Fig. 11 A rough fitting of the RRP -age relationship for the target sample.

Declarations

- Competing interests The authors declare no competing interests.
- Data availability The data in this work are created by cross-matching https://content.cld.iop.org/journals/0067-0049/211/2/24/revision1/apjs492452t1_mrt.txt, *Gaia* DR3 (Epoch 2016), and *Gaia* DR3 Astrophysical params using Topcat [46]. Note that `apjs492452t1_mrt.txt` do not have RA DEC, so cross-matching with https://archive.stsci.edu/pub/kepler/catalogs/kepler_stellar_17.csv.gz using KID first. The “target sample” is filtered by `Mass_Flame>1.2 & Mass_Flame<2`, the main-sequence phase (blue) is filtered further by `(log10(Rad_Flame) < 1.72 * (log10(Mass_Flame) - 0.062) + 0.22)`, and the turn-off phase (red) is filtered further by `(log10(Rad_Flame) >= 1.72 * (log10(Mass_Flame) - 0.062) + 0.22)`.
- Author contributions Y.-F.S is responsible for the data analysis and paper draft. Y.-F.S. also proposed and initiated this research subject. The manuscript was further revised by Y.X., Y.-B.W., X.-L.H., X.-X.H., and Q.Y. with all authors contributing comments and suggestions.

References

- [1] Ferreira, J., Pelletier, G., Appl, S.: Reconnection X-winds: spin-down of low-mass protostars. *Monthly Notices of the Royal Astronomical Society* **312**(2), 387–397

- (2000) <https://doi.org/10.1046/j.1365-8711.2000.03215.x>
- [2] Matt, S., Pudritz, R.E.: The spin of accreting stars: dependence on magnetic coupling to the disc. *Monthly Notices of the Royal Astronomical Society* **356**(1), 167–182 (2005) <https://doi.org/10.1111/j.1365-2966.2004.08431.x> [arXiv:astro-ph/0409701](https://arxiv.org/abs/astro-ph/0409701) [astro-ph]
- [3] Zanni, C., Ferreira, J.: MHD simulations of accretion onto a dipolar magnetosphere. I. Accretion curtains and the disk-locking paradigm. *Astronomy and Astrophysics Review* **508**(3), 1117–1133 (2009) <https://doi.org/10.1051/0004-6361/200912879>
- [4] Matt, S.P., Pinzón, G., de la Reza, R., Greene, T.P.: Spin Evolution of Accreting Young Stars. I. Effect of Magnetic Star-Disk Coupling. *Astrophysical Journal* **714**(2), 989–1000 (2010) <https://doi.org/10.1088/0004-637X/714/2/989> [arXiv:1005.0863](https://arxiv.org/abs/1005.0863) [astro-ph.SR]
- [5] Zanni, C., Ferreira, J.: MHD simulations of accretion onto a dipolar magnetosphere. II. Magnetospheric ejections and stellar spin-down. *Astronomy and Astrophysics Review* **550**, 99 (2013) <https://doi.org/10.1051/0004-6361/201220168> [arXiv:1211.4844](https://arxiv.org/abs/1211.4844) [astro-ph.SR]
- [6] Gallet, F., Bouvier, J.: Improved angular momentum evolution model for solar-like stars. II. Exploring the mass dependence. *Astronomy and Astrophysics Review* **577**, 98 (2015) <https://doi.org/10.1051/0004-6361/201525660> [arXiv:1502.05801](https://arxiv.org/abs/1502.05801) [astro-ph.SR]
- [7] Lin, M.-K., Krumholz, M.R., Kratter, K.M.: Spin-down of protostars through gravitational torques. *Monthly Notices of the Royal Astronomical Society* **416**(1), 580–590 (2011) <https://doi.org/10.1111/j.1365-2966.2011.19074.x> [arXiv:1105.3205](https://arxiv.org/abs/1105.3205) [astro-ph.SR]
- [8] Hartmann, L., Stauffer, J.R.: Additional Measurements of Pre-Main-Sequence Stellar Rotation. *Astronomical Journal* **97**, 873 (1989) <https://doi.org/10.1086/115033>
- [9] Herbst, W., Eislöffel, J., Mundt, R., Scholz, A.: The Rotation of Young Low-Mass Stars and Brown Dwarfs. In: Reipurth, B., Jewitt, D., Keil, K. (eds.) *Protostars and Planets V*, p. 297 (2007). <https://doi.org/10.48550/arXiv.astro-ph/0603673>
- [10] Wolff, S.C., Strom, S.E., Dror, D., Lanz, L., Venn, K.: Stellar Rotation: A Clue to the Origin of High-Mass Stars? *Astronomical Journal* **132**(2), 749–755 (2006) <https://doi.org/10.1086/505534> [arXiv:astro-ph/0604533](https://arxiv.org/abs/astro-ph/0604533) [astro-ph]
- [11] Huang, W., Gies, D.R., McSwain, M.V.: A Stellar Rotation Census of B Stars: From ZAMS to TAMS. *Astrophysical Journal* **722**(1), 605–619 (2010) <https://doi.org/10.1088/0004-637X/722/1/605> [arXiv:1008.1761](https://arxiv.org/abs/1008.1761) [astro-ph.SR]

- [12] Rosen, A.L., Krumholz, M.R., Ramirez-Ruiz, E.: What Sets the Initial Rotation Rates of Massive Stars? *Astrophysical Journal* **748**(2), 97 (2012) <https://doi.org/10.1088/0004-637X/748/2/97> arXiv:1201.4186 [astro-ph.SR]
- [13] Borucki, W.J., Koch, D., Basri, G., Batalha, N., Brown, T., Caldwell, D., Caldwell, J., Christensen-Dalsgaard, J., Cochran, W.D., DeVore, E., Dunham, E.W., Dupree, A.K., Gautier, T.N., Geary, J.C., Gilliland, R., Gould, A., Howell, S.B., Jenkins, J.M., Kondo, Y., Latham, D.W., Marcy, G.W., Meibom, S., Kjeldsen, H., Lissauer, J.J., Monet, D.G., Morrison, D., Sasselov, D., Tarter, J., Boss, A., Brownlee, D., Owen, T., Buzasi, D., Charbonneau, D., Doyle, L., Fortney, J., Ford, E.B., Holman, M.J., Seager, S., Steffen, J.H., Welsh, W.F., Rowe, J., Anderson, H., Buchhave, L., Ciardi, D., Walkowicz, L., Sherry, W., Horch, E., Isaacson, H., Everett, M.E., Fischer, D., Torres, G., Johnson, J.A., Endl, M., MacQueen, P., Bryson, S.T., Dotson, J., Haas, M., Kolodziejczak, J., Van Cleve, J., Chandrasekaran, H., Twicken, J.D., Quintana, E.V., Clarke, B.D., Allen, C., Li, J., Wu, H., Tenenbaum, P., Verner, E., Bruhweiler, F., Barnes, J., Prsa, A.: Kepler Planet-Detection Mission: Introduction and First Results. *Science* **327**(5968), 977 (2010) <https://doi.org/10.1126/science.1185402>
- [14] Koch, D.G., Borucki, W.J., Basri, G., Batalha, N.M., Brown, T.M., Caldwell, D., Christensen-Dalsgaard, J., Cochran, W.D., DeVore, E., Dunham, E.W., Gautier, T.N. III, Geary, J.C., Gilliland, R.L., Gould, A., Jenkins, J., Kondo, Y., Latham, D.W., Lissauer, J.J., Marcy, G., Monet, D., Sasselov, D., Boss, A., Brownlee, D., Caldwell, J., Dupree, A.K., Howell, S.B., Kjeldsen, H., Meibom, S., Morrison, D., Owen, T., Reitsema, H., Tarter, J., Bryson, S.T., Dotson, J.L., Gazis, P., Haas, M.R., Kolodziejczak, J., Rowe, J.F., Van Cleve, J.E., Allen, C., Chandrasekaran, H., Clarke, B.D., Li, J., Quintana, E.V., Tenenbaum, P., Twicken, J.D., Wu, H.: Kepler Mission Design, Realized Photometric Performance, and Early Science. *Astrophysical Journal* **713**(2), 79–86 (2010) <https://doi.org/10.1088/2041-8205/713/2/L79> arXiv:1001.0268 [astro-ph.EP]
- [15] al., G.: The Gaia mission. *Astronomy and Astrophysics* **595**, 1 (2016) <https://doi.org/10.1051/0004-6361/201629272> arXiv:1609.04153 [astro-ph.IM]
- [16] van Leeuwen, F., de Bruijne, J., Babusiaux, C., Busso, G., Castañeda, J., Ducourant, C., Fabricius, C., Hambly, N., Hobbs, D., Luri, X., Marrese, P.M., Mora, A., Muinonen, K., Pourbaix, D., Rimoldini, L., Roegiers, T., Sartoretti, P., Teyssier, D., Ulla, A., Utrilla, E., Vallenari, A., van Leeuwen, M., Altavilla, G., Altmann, M., Álvarez, M.A., Andrae, R., Antoja, T., Antonio, M., Arenou, F., Audard, M., Bailer-Jones, C.A.L., Bakker, J., Balbinot, E., Barache, C., Barblan, F., Bastian, U., Bauchet, N., Bellas-Velidis, I., Bellazzini, M., Berthier, J., Biermann, M., Blomme, R., Bombrun, A., Bossini, D., Brouillet, N., Brown, A., Brugaletta, E., Busonero, D., Butkevich, A., Cacciari, C., Cánovas, H., Cantat-Gaudin, T., Carballo, R., Carnerero, M.I., Carrasco, J.M., Cellino, A., Cheek, N., Clementini, G., Clotet, M., Creevey, O.L., Crowley, C., Dafonte, C., Damerdji, Y., David, M., David, P., Davidson, M., De Angeli, F., De Ridder,

J., De Teodoro, P., Delbó, M., Delchambre, L., Delisle, J.-B., Dell-Oro, A., Dharmawardena, T., Diakité, S., Distefano, E., Drimmel, R., Duran, J., Evans, D.W., Eyer, L., Fabrizio, M., Faigler, S., Fernández-Hernández, J., Figueras, F., Findeisen, K., Fouesneau, M., Frémat, Y., Galluccio, L., Garabato, D., Garcia-Gutierrez, A., Garofalo, A., Gavras, P., Giacobbe, P., Giuffrida, G., Gomel, R., González, Á., González-Núñez, J., Gosset, É., Gracia-Abril, G., Guerra, R., Halbwachs, J.-L., Harrison, D.L., Hatzidimitriou, D., Heiter, U., Helmi, A., Henar Sarmiento, M., Hernandez, J., Hestroffer, D., Hodgkin, S., Holl, B., Hutton, A., Jevardat de Fombelle, G., Jordi, C., Jorissen, A., Katz, D., Khanna, S., Klioner, S., Kordopatis, G., Korn, A.J., Krone-Martins, A., Kruszyńska, K., Lammers, U., Lanzafame, A., Lattanzi, M.G., Le Campion, J.-F., Lebreton, Y., Lebzelter, T., Leccia, S., Leclerc, N., Lecoœur-Taïbi, I., Licata, E., Lindegren, L., Lobel, A., Löffler, W., Manteiga, M., Mantelet, G., Marinoni, S., Marshall, D.J., Martín-Fleitas, J., Masana, E., Masip Vela, A., Mazeh, T., Messineo, R., Michalik, D., Mignard, F., Molinaro, R., Monguió, M., Montegriffo, P., Morel, T., Mowlavi, N., Muraveva, T., Nicolas, C., Nienartowicz, K., Ordenovic, C., Osinde, J., Pailer, F., Pallas-Quintela, L., Panahi, A., Pancino, E., Panem, C., Pauwels, T., Pichon, B., Portell, J., Rainer, M., Raiteri, C.M., Ramos, P., Recio-Blanco, A., Reylé, C., Riello, M., Ríos Diaz, C., Ripepi, V., Riva, A., Rixon, G., Robin, A.C., Romero-Gómez, M., Rowell, N., Rybicki, K.A., Rybizki, J., Sadowski, G., Sáez-Núñez, A., Sahlmann, J., Sanna, N., Sarro Baro, L.M., Schultheis, M., Seabroke, G., Segovia Serrato, J.C., Segransan, D., Siddiqui, H., Siopis, C., Smart, R., Sordo, R., Soubiran, C., Sozzetti, A., Spina, L., Spoto, F., Stephenson, C., Tanga, P., Teixeira, R., Thévenin, F., Torra, F.: Gaia DR3 documentation. Gaia DR3 documentation, European Space Agency; Gaia Data Processing and Analysis Consortium. Online at <https://gea.esac.esa.int/archive/documentation/GDR3/index.html> <https://gea.esac.esa.int/archive/documentation/GDR3/index.html> id. 1 (2022)

- [17] al., G.: Gaia Data Release 3. Summary of the content and survey properties. *Astronomy and Astrophysics* **674**, 1 (2023) <https://doi.org/10.1051/0004-6361/202243940> [arXiv:2208.00211](https://arxiv.org/abs/2208.00211) [astro-ph.GA]
- [18] Irwin, J., Hodgkin, S., Aigrain, S., Hebb, L., Bouvier, J., Clarke, C., Moraux, E., Bramich, D.M.: The Monitor project: rotation of low-mass stars in the open cluster NGC2516. *Monthly Notices of the Royal Astronomical Society* **377**(2), 741–758 (2007) <https://doi.org/10.1111/j.1365-2966.2007.11640.x> [arXiv:astro-ph/0702518](https://arxiv.org/abs/astro-ph/0702518) [astro-ph]
- [19] Cieza, L., Baliber, N.: Testing the Disk Regulation Paradigm with Spitzer Observations. II. A Clear Signature of Star-Disk Interaction in NGC 2264 and the Orion Nebula Cluster. *Astrophysical Journal* **671**(1), 605–615 (2007) <https://doi.org/10.1086/522080> [arXiv:0707.4509](https://arxiv.org/abs/0707.4509) [astro-ph]
- [20] Irwin, J., Hodgkin, S., Aigrain, S., Bouvier, J., Hebb, L., Moraux, E.: The Monitor project: rotation of low-mass stars in the open cluster NGC 2547. *Monthly Notices*

- of the Royal Astronomical Society **383**(4), 1588–1602 (2008) <https://doi.org/10.1111/j.1365-2966.2007.12669.x> arXiv:0711.0329 [astro-ph]
- [21] Irwin, J., Hodgkin, S., Aigrain, S., Bouvier, J., Hebb, L., Irwin, M., Moraux, E.: The Monitor project: rotation of low-mass stars in NGC 2362 - testing the disc regulation paradigm at 5 Myr. *Monthly Notices of the Royal Astronomical Society* **384**(2), 675–686 (2008) <https://doi.org/10.1111/j.1365-2966.2007.12725.x> arXiv:0711.2398 [astro-ph]
- [22] Irwin, J., Aigrain, S., Bouvier, J., Hebb, L., Hodgkin, S., Irwin, M., Moraux, E.: The Monitor project: rotation periods of low-mass stars in M50. *Monthly Notices of the Royal Astronomical Society* **392**(4), 1456–1466 (2009) <https://doi.org/10.1111/j.1365-2966.2008.14158.x> arXiv:0810.5110 [astro-ph]
- [23] Rodríguez-Ledesma, M.V., Mundt, R., Eisloffel, J.: Rotational studies in the Orion Nebula Cluster: from solar mass stars to brown dwarfs. *Astronomy and Astrophysics Review* **502**(3), 883–904 (2009) <https://doi.org/10.1051/0004-6361/200811427> arXiv:0906.2419 [astro-ph.SR]
- [24] Hartman, J.D., Gaudi, B.S., Pinsonneault, M.H., Stanek, K.Z., Holman, M.J., McLeod, B.A., Meibom, S., Barranco, J.A., Kalirai, J.S.: Deep MMT Transit Survey of the Open Cluster M37. III. Stellar Rotation at 550 Myr. *Astrophysical Journal* **691**(1), 342–364 (2009) <https://doi.org/10.1088/0004-637X/691/1/342> arXiv:0803.1488 [astro-ph]
- [25] Meibom, S., Mathieu, R.D., Stassun, K.G.: Stellar Rotation in M35: Mass-Period Relations, Spin-Down Rates, and Gyrochronology. *Astrophysical Journal* **695**(1), 679–694 (2009) <https://doi.org/10.1088/0004-637X/695/1/679> arXiv:0805.1040 [astro-ph]
- [26] Littlefair, S.P., Naylor, T., Mayne, N.J., Saunders, E.S., Jeffries, R.D.: Rotation of young stars in Cepheus OB3b. *Monthly Notices of the Royal Astronomical Society* **403**(2), 545–557 (2010) <https://doi.org/10.1111/j.1365-2966.2010.16066.x> arXiv:0911.3588 [astro-ph.SR]
- [27] Delorme, P., Collier Cameron, A., Hebb, L., Rostron, J., Lister, T.A., Norton, A.J., Pollacco, D., West, R.G.: Stellar rotation in the Hyades and Praesepe: gyrochronology and braking time-scale. *Monthly Notices of the Royal Astronomical Society* **413**(3), 2218–2234 (2011) <https://doi.org/10.1111/j.1365-2966.2011.18299.x> arXiv:1101.1222 [astro-ph.SR]
- [28] Meibom, S., Mathieu, R.D., Stassun, K.G., Liebesny, P., Saar, S.H.: The Color-period Diagram and Stellar Rotational Evolution—New Rotation Period Measurements in the Open Cluster M34. *Astrophysical Journal* **733**(2), 115 (2011) <https://doi.org/10.1088/0004-637X/733/2/115> arXiv:1103.5171 [astro-ph.SR]
- [29] Meibom, S., Barnes, S.A., Latham, D.W., Batalha, N., Borucki, W.J., Koch,

- D.G., Basri, G., Walkowicz, L.M., Janes, K.A., Jenkins, J., Van Cleve, J., Haas, M.R., Bryson, S.T., Dupree, A.K., Furesz, G., Szentgyorgyi, A.H., Buchhave, L.A., Clarke, B.D., Twicken, J.D., Quintana, E.V.: The Kepler Cluster Study: Stellar Rotation in NGC 6811. *Astrophysical Journal* **733**(1), 9 (2011) <https://doi.org/10.1088/2041-8205/733/1/L9> arXiv:1104.2912 [astro-ph.SR]
- [30] Agüeros, M.A., Covey, K.R., Lemonias, J.J., Law, N.M., Kraus, A., Batalha, N., Bloom, J.S., Cenko, S.B., Kasliwal, M.M., Kulkarni, S.R., Nugent, P.E., Ofek, E.O., Poznanski, D., Quimby, R.M.: The Factory and the Beehive. I. Rotation Periods for Low-mass Stars in Praesepe. *Astrophysical Journal* **740**(2), 110 (2011) <https://doi.org/10.1088/0004-637X/740/2/110> arXiv:1107.4039 [astro-ph.SR]
- [31] Henderson, C.B., Stassun, K.G.: Time-series Photometry of Stars in and around the Lagoon Nebula. I. Rotation Periods of 290 Low-mass Pre-main-sequence Stars in NGC 6530. *Astrophysical Journal* **747**(1), 51 (2012) <https://doi.org/10.1088/0004-637X/747/1/51> arXiv:1112.2211 [astro-ph.SR]
- [32] Moraux, E., Artemenko, S., Bouvier, J., Irwin, J., Ibrahimov, M., Magakian, T., Grankin, K., Nikogossian, E., Cardoso, C., Hodgkin, S., Aigrain, S., Movsesian, T.A.: The Monitor Project: stellar rotation at 13 Myr. I. A photometric monitoring survey of the young open cluster h Persei. *Astronomy and Astrophysics Review* **560**, 13 (2013) <https://doi.org/10.1051/0004-6361/201321508> arXiv:1306.6351 [astro-ph.SR]
- [33] Cohen, O., Drake, J.J.: A Grid of MHD Models for Stellar Mass Loss and Spin-down Rates of Solar Analogs. *Astrophysical Journal* **783**(1), 55 (2014) <https://doi.org/10.1088/0004-637X/783/1/55> arXiv:1309.5953 [astro-ph.SR]
- [34] Hansen, C.J., Kawaler, S.D., Trimble, V.: *Stellar Interiors : Physical Principles, Structure, and Evolution*, (2004)
- [35] McQuillan, A., Mazeh, T., Aigrain, S.: Rotation Periods of 34,030 Kepler Main-sequence Stars: The Full Autocorrelation Sample. *Astrophysical Journals* **211**(2), 24 (2014) <https://doi.org/10.1088/0067-0049/211/2/24> arXiv:1402.5694 [astro-ph.SR]
- [36] Claret, A., Gimenez, A.: The moment of inertia of main sequence stars. *Astronomy and Astrophysics Supplement Series* **81**(1), 37–45 (1989)
- [37] Howe, R., Christensen-Dalsgaard, J., Hill, F., Komm, R.W., Larsen, R.M., Schou, J., Thompson, M.J., Toomre, J.: Dynamic Variations at the Base of the Solar Convection Zone. *Science* **287**(5462), 2456–2460 (2000) <https://doi.org/10.1126/science.287.5462.2456>
- [38] Ibata, R.A., Lewis, G.F., Irwin, M.J., Quinn, T.: Uncovering cold dark matter halo substructure with tidal streams. *Monthly Notices of the Royal Astronomical Society* **332**(4), 915–920 (2002) <https://doi.org/10.1046/j.1365-8711.2002.05358>

x [arXiv:astro-ph/0110690](https://arxiv.org/abs/astro-ph/0110690) [astro-ph]

- [39] Johnston, K.V., Spergel, D.N., Haydn, C.: How Lumpy Is the Milky Way’s Dark Matter Halo? *The Astrophysical Journal* **570**(2), 656–664 (2002) <https://doi.org/10.1086/339791> [arXiv:astro-ph/0111196](https://arxiv.org/abs/astro-ph/0111196) [astro-ph]
- [40] Carlberg, R.G.: Dark Matter Sub-halo Counts via Star Stream Crossings. *The Astrophysical Journal* **748**(1), 20 (2012) <https://doi.org/10.1088/0004-637X/748/1/20> [arXiv:1109.6022](https://arxiv.org/abs/1109.6022) [astro-ph.CO]
- [41] Ibata, R., Malhan, K., Martin, N., Aubert, D., Famaey, B., Bianchini, P., Monari, G., Siebert, A., Thomas, G.F., Bellazzini, M., Bonifacio, P., Caffau, E., Renaud, F.: Charting the Galactic Acceleration Field. I. A Search for Stellar Streams with Gaia DR2 and EDR3 with Follow-up from ESPaDOnS and UVES. *The Astrophysical Journal* **914**(2), 123 (2021) <https://doi.org/10.3847/1538-4357/abfcc2> [arXiv:2012.05245](https://arxiv.org/abs/2012.05245) [astro-ph.GA]
- [42] Belokurov, V., Erkal, D., Evans, N.W., Koposov, S.E., Deason, A.J.: Co-formation of the disc and the stellar halo. *Monthly Notices of the Royal Astronomical Society* **478**(1), 611–619 (2018) <https://doi.org/10.1093/mnras/sty982> [arXiv:1802.03414](https://arxiv.org/abs/1802.03414) [astro-ph.GA]
- [43] Johnson, D.R.H., Soderblom, D.R.: Calculating Galactic Space Velocities and Their Uncertainties, with an Application to the Ursa Major Group. *The Astronomical Journal* **93**, 864 (1987) <https://doi.org/10.1086/114370>
- [44] McMillan, P.J.: The mass distribution and gravitational potential of the Milky Way. *Monthly Notices of the Royal Astronomical Society* **465**(1), 76–94 (2017) <https://doi.org/10.1093/mnras/stw2759> [arXiv:1608.00971](https://arxiv.org/abs/1608.00971) [astro-ph.GA]
- [45] Marks, M., Kroupa, P., Dabringhausen, J., Pawlowski, M.S.: Evidence for top-heavy stellar initial mass functions with increasing density and decreasing metallicity. *Monthly Notices of the Royal Astronomical Society* **422**(3), 2246–2254 (2012) <https://doi.org/10.1111/j.1365-2966.2012.20767.x> [arXiv:1202.4755](https://arxiv.org/abs/1202.4755) [astro-ph.GA]
- [46] Taylor, M.B.: TOPCAT & STIL: Starlink Table/VOTable Processing Software. In: Shopbell, P., Britton, M., Ebert, R. (eds.) *Astronomical Data Analysis Software and Systems XIV*. *Astronomical Society of the Pacific Conference Series*, vol. 347, p. 29 (2005)